We are IntechOpen, the world's leading publisher of Open Access books Built by scientists, for scientists

6,900
Open access books available

186,000
International authors and editors

200M
Downloads

Our authors are among the

154
Countries delivered to

TOP 1%
most cited scientists

12.2%
Contributors from top 500 universities

WEB OF SCIENCE™

Selection of our books indexed in the Book Citation Index in Web of Science™ Core Collection (BKCI)

Interested in publishing with us?
Contact book.department@intechopen.com

Numbers displayed above are based on latest data collected.
For more information visit www.intechopen.com

3

An Improved Method of Fabricating Rare Earth Doped Optical Fiber

Ranjan Sen and Anirban Dhar
CSIR-Central Glass & Ceramic Research Institute, Kolkata, India

1. Introduction

Optical fiber, a technology well-known to have revolutionized the telecommunication industry, is now becoming the key component behind the success of a number of enabling technologies such as sensing, biomedicine, defence, security and novel light sources. Along with standard telecommunication fibers, rare earth (RE) doped specialty optical fibers are the backbones of the photonics industry. Elements such as erbium (Er), ytterbium (Yb), yttrium (Y), neodymium (Nd), thulium (Tm) and europium (Eu) are vital optically active ingredients at the heart of many lasers, optical amplifiers and phosphors. Erbium-doped fiber amplifier (EDFA) — to overcome losses in long-distance optical communication links, fiber lasers — a technology having great potential for medical, defence and manufacturing sectors, Light Emitting Diode (LED) - across the visible, ultraviolet and infrared wavelengths, potential for vast range of applications like traffic signals, instrumentation, communication, televisions, display etc. are just a few obvious examples. A range of optical fiber designs and materials are now being developed to meet the needs of both established and growing industries.

Several research groups and industries around the world are developing the technology required to fabricate RE doped fibers with enhanced performance. In contrast to the standard telecommunication fibers, active fibers demand a greater variety of materials and structures in order to realize superior characteristics of amplification and lasing at a variety of operating wavelengths. Thus an optimized fabrication process needs to be established.

Out of the various processes used for manufacturing optical fibers, the Modified Chemical Vapor Deposition (MCVD) process [Nagel et al. 1982, MacChesney, 2000] has been widely accepted for making specialty fibers because of better control over refractive index (RI) profile and superior process flexibility. In this process, the reactant gases ($SiCl_4$, O_2 and various dopant precursors) passing down a rotating silica tube is heated by an external oxy-hydrogen burner that slowly traverses in the direction of input gas flow. The proportion of $SiCl_4$ and the dopants is precisely controlled by controlling the amount of carrier gas (mostly oxygen) through the bubblers containing liquid halide precursors having reasonably high vapor pressure (~10^2 mm of Hg) over the temperature range of 20-30°C. The reactant gases undergo high-temperature oxidation to form submicrometer range soot particles which get deposited downstream of the hot zone according to thermophoretic mechanism [Li, 1985]. The particulate layer is consolidated into thin pore free glassy film as the burner traverses over the deposited region. The desired RI profile is built up by repeating the above step with variation of vapor phase composition. Subsequent to completion of deposition, the tube is

collapsed to a solid rod, known as preform through a few passes of the burner at temperatures above 2000°C.

The above technique is however not suitable for doping RE inside the preform core due to low vapor pressure of the RE precursors [Digonnet, 1993] at temperatures of 20-30°C. Thus RE doped fibers are prepared by modifying standard fabrication processes and adopting special techniques. The MCVD coupled with RE-doping process viz. solution doping method [Stones & Burrus, 1973; Townsend et.al 1987], sol-gel process [Matjec et al. 1997; Chatterjee et al. 2003] and direct nano-particle deposition (DND) [Tammela et al. 2002] are some of the well known methods that have been exploited successfully. On the contrary, the vapor phase delivery techniques namely heated frit source delivery [Ainslie et al. 1988], heated source delivery [Poole, 1985, 1986], heated source injector delivery [MacChesney & Simpson, 1985], aerosol delivery [Laoulacine et al. 1988; Morse et al. 1989], chelate delivery method [Thompson et al. 1984; Tumminelli et al. 1990], which require relatively complex set-up and have not yet been standardized for commercial production.

Since its inception, solution doping process has been well accepted due to its process simplicity and low implementation cost for fabricating RE-doped preforms among the various known methods. Although, MCVD coupled with solution doping is now well established and regularly employed even for commercial fiber production, the process still suffers from poor control over RE incorporation and reproducibility. The non-uniform thickness, porosity and pore size distribution in the deposited core layer leads to variation in RE concentration and inhomogeneity along the length of the preform/fiber. On the other hand solution strength, Al/RE proportion, dipping period etc influence the RE incorporation and fiber properties during solution doping stage. Thus judicious adjustment of the different process parameters based on their interdependence is vital for any further improvement in the process and the fiber performance. Till date no detailed exercise has been done to achieve such process optimization. Unless one understands the effect and interrelation of different process steps involved in the solution-doping technique it is not feasible to get control over the entire process.

This Chapter describes a systematic investigation on the process steps and associated parameters related to the above concerns. The experimental methodologies for optimization of soot deposition conditions and solution doping parameters are reported with important results. The correlation of soot morphology and solution parameters with ultimate fiber properties is presented along with optimized fabrication conditions which led to about 80% process reproducibility.

2. MCVD-solution doping process

MCVD process coupled with solution doping technique involves two major steps, viz. deposition of porous core layer within a silica tube using MCVD process at appropriate deposition temperature and impregnation of the porous deposit with a solution containing salts of RE (or combination of REs) and a codopant, mostly Al. The soaked layer is gently heated in presence of oxygen for conversion of the RE- and Al-salts into oxides. This is done to avoid evaporation of the salts during subsequent processing stages at high temperature and reduction of the RE content in the core in an uncontrolled manner. However, control of temperature at this stage is critical to ensure complete oxidation without evaporation which is strongly dependent on the characteristics of the salt used. The porous layer is subsequently dehydrated in presence of chlorine to eliminate OH adsorbed in the soot during solution doping. A temperature between 800-1200°C is usually maintained at this

stage. However the duration needs to be optimized based on the thickness of the porous layer. The final step is sintering of the layer to obtain the RE doped core. A slow sintering process comprising several passes of the burner and gradual increase of temperature is helpful [Bandyopadhyay et al. 2001] to ensure smooth sintering without formation of imperfections within the sintered layer. The tube containing the RE-doped core is finally collapsed to produce the preform. A soft collapsing technique like the method adopted during sintering is useful to avoid loss of RE and Al-oxides from the core, particularly from the innermost region causing a central dip. The technique also provides preforms with good geometry. Fibers of desired dimension with resin coating are drawn under optimum conditions using a fiber drawing tower to achieve the desired optical and mechanical properties. A schematic of the solution doping method is shown in Fig. 1.

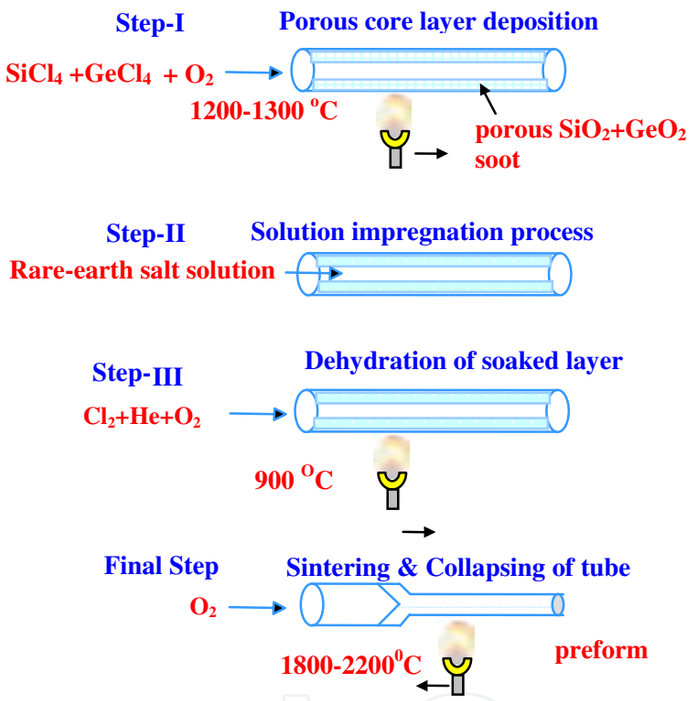

Fig. 1. Schematic of MCVD-solution doping process.

The critical step in this process is the deposition of uniform soot layer of suitable composition and porosity which serves as the precursor for solution impregnation. The variation in porosity as well as the pore size distribution leads to poor control over RE incorporation and inhomogeneity along the length of the preform/fiber. As a result, identical lengths of fiber from different sections of the preform do not provide the same performance. Unless the soot layer morphology is completely known and can be controlled by suitably adjusting the deposition conditions, the fiber performance cannot be improved. On the other hand the composition of the soaking solution, the Al/RE ratio, the nature of solvent, etc. are the controlling factors during the solution doping step to achieve the desired properties in the fiber.

Keeping in view the above factors, experiments have been performed on two broad aspects: a) control of soot deposition following MCVD process and b) optimization of solution doping parameters subsequent to deposition. This is elaborated in the following two

sections. Each section consists of experimental methodology, characterization procedures adopted and significant observations with optimized conditions achieved. The results of the two parts are ultimately combined to realize the optimized fabrication conditions that enable to achieve enhanced repeatability with good control over RE incorporation.

3. Optimization of soot deposition parameters

In this section the influence of parameters controlling soot layer morphology is discussed. Two important parameters namely vapor phase composition and soot deposition temperature have been identified for an in-depth study to correlate their influence on the porous deposit microstructure and consequent effect on final preform/fiber characteristics. The soot layer characteristics have been critically analyzed and results obtained are correlated with the experimental parameters to achieve optimized deposition conditions.

3.1 Experimental methodologies

3.1.1 Soot composition

The MCVD process was adopted to deposit porous silica layers of various compositions at selected temperatures inside a 20 mm outer diameter silica tube (F-300 grade from Heraeus) with tube thickness of 1.25 mm. In order to investigate the effect of vapor phase composition on deposited soot layer morphology, three different vapor phase compositions, specifically pure SiO_2, SiO_2+GeO_2 ($GeCl_4/SiCl_4$=0.86) and SiO_2+P_2O_5 ($POCl_3/SiCl_4$=0.48) were selected. A temperature in the range of 1200-1300°C was selected for depositing pure SiO_2 and SiO_2+GeO_2 layers. Since at this temperature SiO_2+P_2O_5 soot starts sintering, a temperature close to 1100°C was selected for depositing SiO_2-P_2O_5 composition which enabled to obtain soot layer with appreciable porosity for the selected vapor phase composition. Except a lower deposition temperature in case of SiO_2-P_2O_5, the other experimental conditions remained same for all the compositions.

Following the soot deposition, solution impregnation was carried out for fixed time span of 1 hour using an ethanolic solution containing 0.3 M $AlCl_3$ + 0.01 M $ErCl_3$. The soaked soot deposit was then oxidized and dehydrated. The dehydration was carried out in presence of Cl_2 at a temperature of 900°C. The oxidized layer was sintered in presence of O_2 and helium at temperatures in the range of 1400°C to 1700°C. Finally collapsing was performed at a temperature above 2200°C to obtain the preform. Fibers of 125±0.2 μm diameter with dual resin coating were drawn from the preforms in a conventional tower (Heathway, UK make).

3.1.2 Soot deposition temperature

In order to examine the influence of deposition temperature on the porous deposit characteristics as well as the ultimate fiber properties in terms of RE incorporation, another series of experiment was carried out. In this series GeO_2 doped porous core layer was deposited at temperatures of 1220, 1255 & 1295°C maintaining the same vapor phase composition ($GeCl_4/SiCl_4$=0.86). The deposited soot was then processed following similar experimental conditions mentioned above (Sec 3.1.1) to obtain the final preform/fiber and to characterize their properties.

3.2 Characterization procedure

Scanning electron microscope (SEM Model:LEO-S430i) has been extensively used to analyze deposited soot morphology with variation of composition and deposition temperature. The

samples of deposit were collected from different sections of the overall length of tube both before and after solution doping in a careful manner to preserve the soot structure and avoid generation of defects. The selected specimens were dried under infra-red (IR) lamp for about 30 minutes to remove adsorbed moisture from the soot surface and coated with silver (Ag) using EMSCOPE (UK made) DC sputtering instrument prior to SEM investigation. Both secondary electron (SE) and back scattered electron (BSE) images were captured based on the required information. An image analysis software (LEICA Q500Mc) was utilized to calculate size and shape of the pores within the soot deposited from captured SEM images.

In order to correlate the results obtained from the SEM micrograph analysis, surface area measurement was performed for different soot samples following BET (Brunaur-Emmett-Teller) method to get an idea about the sizes of pores formed within the soot deposit. Accordingly, samples of soot deposit were collected from the substrate tube by taking utmost care to avoid any damage in soot structure. The samples were dried by heating around 100°C and precise weight was taken before putting inside the instrument (Quantachrome). Liquid Nitrogen gas was used as an adsorbate. The sample weight was varied from 0.05 gm to 0.15 gm in different measurement to check the repeatability of the result obtained.

The composition of collected soot deposit before solution doping had been determined using chemical analysis technique. This was specially aimed for Ge and P doped soot in order to compare the composition of deposited soot layer with that of input vapor mixture and sintered core in the final preform. Usually Inductively Coupled Plasma (ICP) method was used to determine the soot composition, but for Ge doped soot particles, besides ICP, a special analytical method [Mukhopadhyay & Kundu, 2006] using mannitol as complexing agent has been developed. This alternative technique provides very good result for the soot samples and matches closely with result obtained from ICP method.

The Electron Probe Micro Analysis (EPMA) of the polished preform samples was carried out using JEOL 8900 Electron Probe Microanalyzer to determine the RE and Al distribution across the core of the preform sample. For this investigation preform samples of 1.5 mm thickness polished on both the faces were prepared and measurements were carried out across the preform core at an interval of 5 μm to acquire the data on elemental distribution.

Longitudinal and radial homogeneity of the fabricated preforms in terms of RI were evaluated using preform analyzer (PK2600). Similarly employing fiber analyzer (NR20, EXFO), RI profile and numerical aperture (NA) of the drawn fiber were analyzed. The attenuation of the fabricated fibers was measured using "cutback technique" employing spectral attenuation measurement set-up (Bentham, UK-made). The measurement was carried out in a spectral range of 800 nm to 1600 nm. Fibers drawn from different parts of the preform were measured and compared for verifying compositional uniformity and repeatability of measurement.

3.3 Results & discussion

3.3.1 Pore size vs soot composition

The SEM investigation of porous soot deposit reveals interdependence of soot layer morphology and layer thickness with input vapor phase composition. The addition of Ge or P-oxide is found to influence the particle growth dynamics and the viscosity of the silicate, which control the formation of the deposited soot network. With the lowering of viscosity, the porous structure collapses and unites together more easily, forming larger pores even at lower temperatures besides reducing deposited layer thickness. The SEM micrographs

presented in Fig. 2 show the change in porous layer microstructure with change in soot composition. Pure SiO_2 deposit is homogeneous with finer network structure while the SiO_2+P_2O_5 network is composed of pores with wide variation in shape and size. Such variation is a consequence of pore collapsing and combining together as P facilitates sintering at lower temperature. The GeO_2 doped deposit has an intermediate structure between SiO_2 and SiO_2+P_2O_5 composition. Image analysis result shown in Fig. 2 represents the variation in pore size distribution in relation to soot composition. Accordingly the mean pore size is found to be 0.5 μm for SiO_2, 1.5 μm for SiO_2+GeO_2 and 5.5 μm for SiO_2+P_2O_5 soot samples. The observations indicate that pure SiO_2 deposit is most suitable for using as a precursor during solution doping as the network homogeneity and pore size uniformity are superior compared to other compositions. However, experiments reveal that pure SiO_2 deposit has the disadvantage of disengaging during soaking due to poor adhesion with the silica tube surface. So the amount of dopant in the soot deposit and the deposition temperature needs to be judiciously selected to achieve good compositional homogeneity.

The gradual addition of dopants such as GeO_2 and P_2O_5 led to decrease in the thickness compared to that of pure SiO_2 layer due to lowering of viscosity and sintering temperature, which results in densification of the layer. The thickness is least (mostly below 5 μm) for P-doped soot layer as P facilitates the sintering appreciably and highest for pure SiO_2 soot layer. In the case of GeO_2 doped soot layer, the thickness varied from 3.5 μm to 7.5 μm corresponding to change in temperature from 1295°C to 1255°C.

A new term 'pore area fraction' proposed in this regard and defined by the ratio of total pore area to the area of the deposit under consideration, showed a variation of 50% to 8% for the different compositions. The analytical data are presented in Table 1.

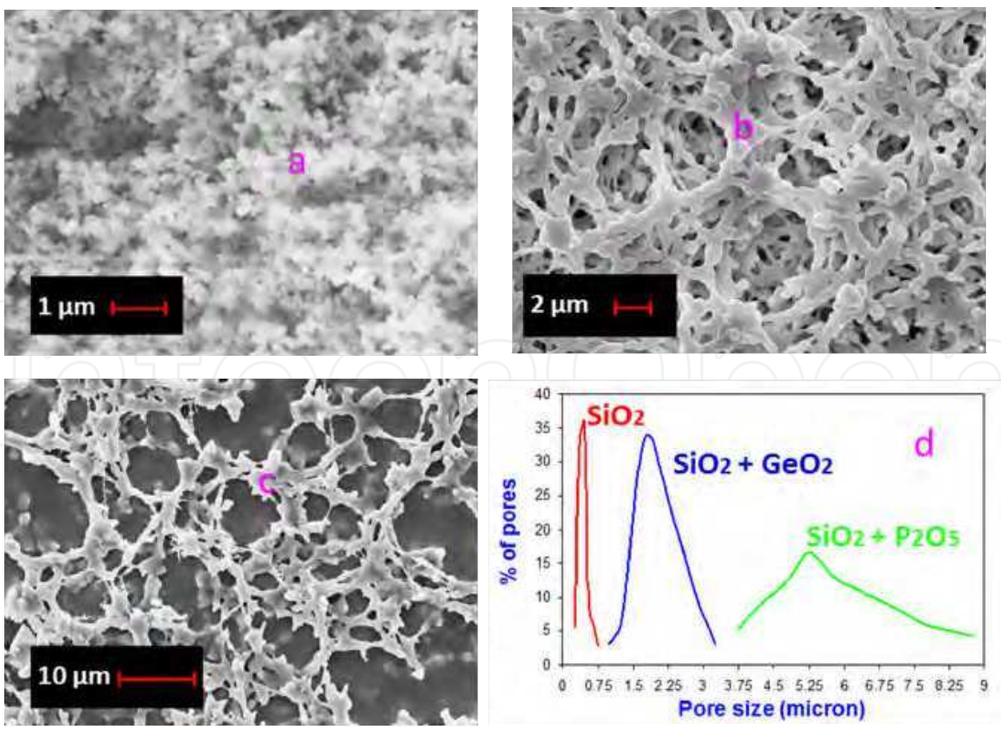

Fig. 2. SEM micrograph of (a) pure SiO_2, (b) GeO_2 doped, (c) P_2O_5 doped soot and (d) pore size distribution with change in soot composition.

Deposition temperature (°C)	Vapor phase composition	Average pore size in μm	Pore area fraction
1250	Pure SiO_2	0.3-0.5	8%
1250	SiO_2+GeO_2	1.5-2.0	27%
1100	SiO_2+P_2O_5	5.0-5.5	50%

Table 1. Variation of pore sizes with change in composition.

3.3.2 Pore size vs. soot deposition temperature

The SEM micrograph of GeO_2 doped soot layers deposited at temperatures of 1220° and 1295°C is presented in figs. 3 (a) & (b). Comparison of the said micrographs clearly reveals strong influence of deposition temperature over the network formation of the soot particles and the pore size distribution. The pore size distribution evaluated from image analysis of the micrographs provides a quantitative comparison as shown in Fig. 3 (c). The curves in the Fig.3 (c) represent pore size analysis of the soot deposit at temperatures of 1255°and 1295°C respectively. It is observed that the pore size has a wider distribution at higher temperature although mean pore size remains in the range of 1.5 μm. Thus at higher temperature the pores seem to collapse and fuse together resulting in greater pore size variation and decrease in porosity due to partial consolidation. If the number of pores in the range of 1-2 μm is taken as an indicator of uniformity, it is observed that the uniformity of pore size distribution reduces from 70% to 59% corresponding to the above temperature increment of 75°C. The pore area fraction showed a variation of 32% to 24% for the said increase in temperature from 1255° to 1295°C.

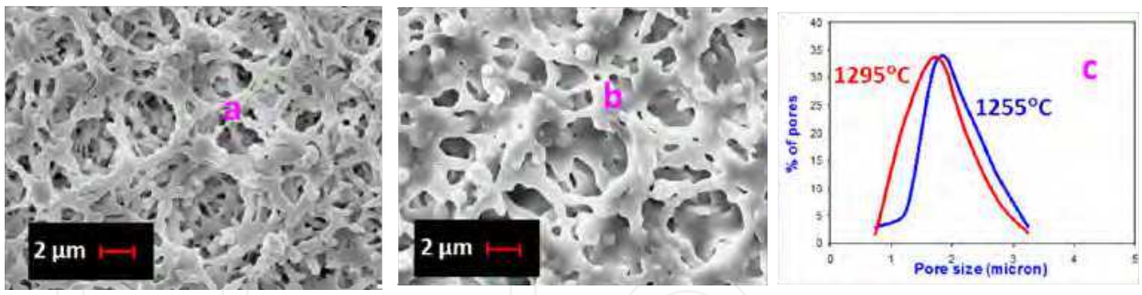

Fig. 3. SEM micrograph (a) SiO_2-GeO_2 soot deposited at 1220°C, (b) SiO_2-GeO_2 soot deposited at 1295°C and (c) Pore size distribution against deposition temperature for SiO_2-GeO_2 doped soot at 1255°C and at 1295°C.

3.3.3 Effect of composition and deposition temperature on surface area

The analysis of surface area of the soot particles is found to be in good agreement with interpretation drawn from SEM analysis as already discussed. The surface area of pure SiO_2 soot is about 195 m^2/g at 1200°C and decreases significantly with addition of dopant like Ge or P. About 2 to 3 folds enhancement in surface area is observed irrespective of soot composition for a 55°C reduction in deposition temperature as evidenced by result given in Table 2. This reduction is a result of partial consolidation of the soot layer at higher temperatures. On the other hand, the reduction in soot layer viscosity with addition of dopant like Ge or P is the reason behind lower surface area of doped silicate soot layer compared to pure silica.

Soot composition	Deposition temperature (°C)	Surface area, m^2/g
SiO_2	1200	195.01
	1255	66.79
SiO_2+GeO_2 ($GeCl_4/SiCl_4$ =0.86)	1200	18.07
	1255	10.32
SiO_2+P_2O_5 ($POCl_3/SiCl_4$=0.48)	1100	8.8

Table 2. Surface area of soot samples of different compositions.

3.3.4 Composition of soot and its influence

Chemical analysis of soot deposit when compared to input vapor composition and final core composition provides important information related to process mechanism involved during processing of soot deposit subsequent to solution soaking. GeO_2 proportion in the soot corresponds to about 73% and 81% completion of oxidation reaction of $GeCl_4$ at core deposition temperatures of 1250°C and 1295°C respectively. The values are found to be in close proximity to the theoretically calculated conversion of 82% and 87% at the said temperatures. The theoretical analysis has been done by considering the reaction as first order with respect to the chloride reactant and evaluating the rate constant values at specific temperatures [Pal et al. 2005]. The similarity of GeO_2 proportion in the input vapor mixture with that in the unsintered soot layer is significant as it is directly related to the viscosity of the deposit and the extent of sintering at the deposition temperature. The NA of the ultimate fiber corresponding to this composition is near to 0.20 which corresponds to 10.5 mol% GeO_2 in the core. Thus the GeO_2 content in soaked soot substantially decreases in the ultimate core layer indicating that the major amount of GeO_2 is lost during sintering and collapsing stages. The result reveals that the network formation and pore collapsing take place in soot with much higher GeO_2 concentration than that present in the final fiber. Similar result was obtained while analyzing the soot containing P_2O_5 where the problem of evaporation is more pronounced.

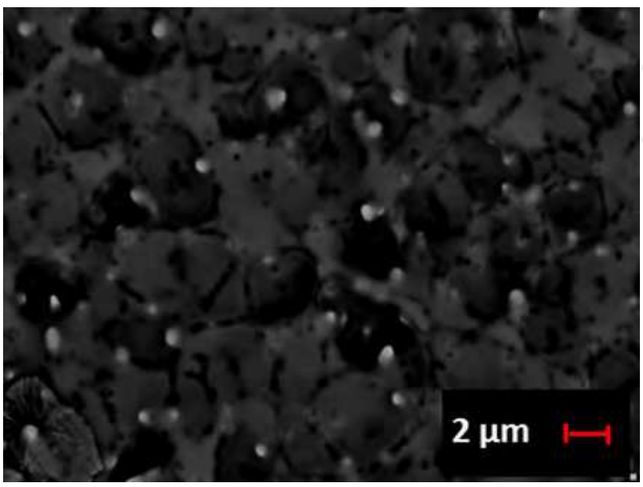

Fig. 4. SEM micrograph of SiO_2-GeO_2 soot deposited at 1295°C after solution doping.

3.3.5 RE incorporation dependence on soot composition and deposition temperature

The BSE micrograph of the SiO_2+GeO_2 layer subsequent to soaking with a solution of 0.3 M $AlCl_3$ + 0.01 M $ErCl_3$ in ethanol for one hour is presented in Fig. 4. The solution impregnation through the pores is prominent with white region in the image showing the presence of higher molecular weight substances like Er (white) and Al (grey). The point that is evident is that the uniformity of dopant impregnation through solution is dependent on the morphology of the soot layer deposit. Larger pores draw greater amount of solution leading to increase in both RE and Al concentration and consequently act as precursor for development of RE and Al clusters. It is known that RE clustering leads to pair induced quenching and degradation in final fiber performance. Similarly the Al clusters are also probable sources for Al rich phase separation and defect generation in the core. Thus a uniform pore size distribution is a prerequisite to obtain uniform RE distribution in the ultimate preform/fiber.

The analysis of SEM images and surface area results indicates that pure silica soot network consists of smaller pores with higher surface to volume ratio compared to doped silica soot deposit. Accordingly based on the soot porosity and pore size uniformity factor, pure silica stands as the preferred soot composition to obtain RE-doped preforms with uniform distribution along the length compared to Ge or P doped core layer. However, weak adhesion of pure SiO_2 deposit with the silica tube surface is associated with the risk of peeling off during soaking (particularly for solution of higher concentration) besides poor RE solubility. All these restrict the use of pure silica as the core layer composition. Considering essential requirement of RE doped fibers and analyzing the above results, GeO_2-doped silica soot is found to be the most suitable for formation of core layer and a deposition temperature of 1260°C is found to be optimum to obtain acceptable pore size uniformity for the selected vapor phase composition.

A correlation has been worked out with regard to final Er incorporation in three different soot layers deposited with variation in temperature and composition. The absorption at 980 nm due to Er content differs by about 0.90 dB/m for two GeO_2 doped fibers where the deposition temperatures had a difference of 40°C [Dhar et al. 2006]. This corresponds to an Er concentration difference of 200 ppm. The fiber F1 prepared using lower soot deposition temperature (1255°C) has higher absorption compared to fiber F2 prepared from soot deposited at 1295°C as shown in Fig.5. Thus a concentration difference of 100 ppm is observed for a temperature variation of 20°C for the selected composition. Partial sintering with collapsing of the pores at higher temperature leads to reduced surface to volume ratio and consequently less solution retention resulting in lesser incorporation of rare earth ion. The observation is important to optimize the solution doping parameters and control RE concentration in the fiber. However, P_2O_5 doped soot demonstrates reverse trend and the fabricated fibers contain higher Er concentration instead of soot layer densification due to viscosity lowering and reduced intake of solution. This reverse trend can be explained on the basis of the soot chemistry of Si-P [Digiovanni et al. 1989] in comparison to that of Si-Ge. Substitution of Si by P helps to avoid charge imbalance, which results in additional Al absorption and consequent increases in Er level in the layer. Additionally investigation of the soot network structure indicates that P doped layer contains larger pores compared to the Ge doped deposit and has the capacity of retaining more amount of solution. This is because in case of P addition, the pores have a tendency to combine together with the disappearance of intermediate wall during partial consolidation instead of mere size reduction.

An interesting empirical relation has been established analyzing the results on soot morphology in terms of pore area fraction and Er ion incorporation level. The absorption of 3.12, 2.27 and 4.99 dB/m (Table 3) is observed against pore area fraction of 32%, 24% and 50% in the porous layer microstructures of fibers F1, F2 and F3 respectively. This corresponds to a relation of B=c.Q, where B represents Er ion absorption at 980 nm in dB/m, Q the percent pore area fraction and c is a constant. The value of c is found to be 0.1 for the solution used in the present case. The relation is found to be valid for several fibers fabricated for this purpose. The point that is obvious from all the above results is that an analysis of the porous layer microstructure provides an indication about the rare earth concentration, distribution and the homogeneity in the final preform/fiber.

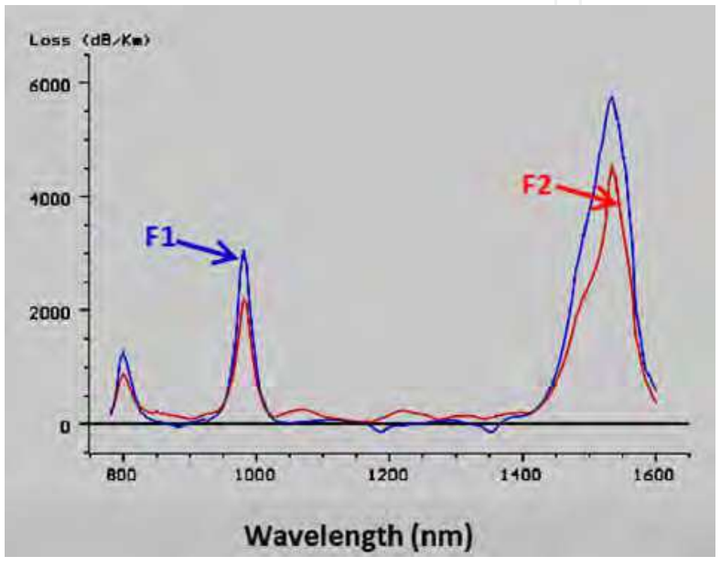

Fig. 5. Spectral attenuation curves of F1 and F2 showing Er^{3+}concentration variation.

Fiber	Input vapor mixture	Deposition temperature (°C)	Er ion absorption peak at 980 nm, dB/m	Fiber Characterization	
				NA	Core-diameter in μm
F1	$GeCl_4/SiCl_4$=0.86	1255	3.120	0.22	7.6
F2	$GeCl_4/SiCl_4$=0.86	1295	2.265	0.20	7.5
F3	$POCl_3/SiCl_4$=0.48	1100	4.990	0.13	6.5

Table 3. Fiber properties and parameters.

4. Solution doping parameters

During the solution doping phase, there are a number of parameters which play a significant role. In this section we have identified the parameters which are important for

controlling solution impregnation and consequently RE/Al incorporation into the core which determine the final fiber performance. Emphasis is given on optimization of solution doping parameters and correlation with soot characteristics to achieve enhanced process repeatability.

4.1 Solution doping parameters

The SEM images of soot deposit clearly show that the porous layer comprises of open or closed pores interconnected to form 3-dimensional structures. Although the nature of network and extent of open and closed pores depend on soot-composition and chosen deposition temperature, the soot structure can be seen as series of capillaries interconnected to each other with irregular arrangement. Thus during solution doping the flow through this porous layer is equivalent to flow of soaking solution through capillaries. It is well known that the flow of solution through porous medium is inversely proportional to solution viscosity as demonstrated by the following equation:

$$V = \frac{r}{4\mu l}\gamma\cos\theta \tag{1}$$

where V = velocity of solution flowing through porous medium
r = radius of capillary tube (can be taken as pore size), l = length of porous frit,
μ = viscosity of solution, γ = surface tension of liquid, θ = contact angle
Thus the solution viscosity and surface tension are critical factors to achieve desired dopant incorporation into the preform core. Both the parameters are dependent on the selected solution composition. According to equation (1), higher viscosity of the solution leads to reduction in flow through the pores. Therefore, the dipping period assumes significant importance according to solution properties for desired RE doping in the core. The other important parameters are RE-salt concentration and proportion of Al/RE in the solution. It is well known that Al codoping helps in solvation of RE ions in silica network [Arai et al. 1986] and reduces the loss of RE from the core during collapsing stages [Ainslie et al. 1988]. Although it is established that increased dopant concentration in the solution leads to higher dopant intake into the core, the proportion of Al/RE needs to be optimized to avoid unwanted clustering effect which degrades final fiber performance. The core-clad interface also shows defect generation when the preform core is rich in Al_2O_3 which increases scattering loss of the fiber. Accordingly a systematic investigation was carried out to achieve optimized soaking solution composition and process conditions during solution impregnation stage. Experimental methodologies used, characterization techniques employed and results obtained are discussed in the following sub-sections.

4.2 Experimental methodologies

4.2.1 Solution properties

The viscosities of solutions with varying dopant concentrations prepared using different solvents viz. water, methanol, ethanol and n-propanol were measured for comparison and establishing a database which can be utilized for selection of appropriate solvent and concentration during preparation of the soaking solution. Al ion concentration was varied from 0.15 M to 0.98 M keeping RE ion concentration fixed at 0.01 M. Either $AlCl_3$ or $Al(NO_3)_3$ was used as a source of Al-salt while $ErCl_3$ was the RE ion source in these experiments. The density and viscosities of different soaking solutions was measured using

pycnometer and Ostwald Viscometer at 25°C while surface tension value was taken using "du Nouy Tensiometer" at 25°C.

4.2.2 Selection of solvent

The solvent used for preparation of soaking solution, should be polar in nature with appreciable dielectric constant in order to dissolve Al and RE salt easily, it must be low boiling liquid so that evaporates easily on passing inert gas like N_2 at room temperature after solution doping and should not chemically react with deposited soot layer. These requirements restrict the choice of solvent to water and alcohol. In order to assess the effect of solvent on final fiber performance, we fabricated a series of preforms where two parts were soaked with soaking solution of same strength but dissolved using either water or ethanol.

For this investigation a 60 cm long wave guide tube (Suprasil F-300) of dimension 20/17.5 mm was selected and porous core layer of optimized GeO_2-doped silica soot (already discussed under section 3) was deposited at a temperature region of 1255^{o}C subsequent to deposition of F-doped cladding layers. The deposited tube was then cut into two equal parts and separately dipped for one hour into two different soaking solutions containing 0.3 M $AlCl_3$+0.01 M $ErCl_3$ prepared using water and ethanol as solvent. Subsequent to solution doping, two parts were remounted on the glass working lathe, joined and processed further to obtain the final preform. Thus the preform fabricated consists of two parts soaked with ethanolic and aqueous solutions. Fibers were drawn from two ends of the preform and Er-incorporation was compared to investigate the influence of solvent effect.

4.2.3 Influence of dipping period

In order to investigate the effect of dipping period, we carried out the experiment using optimized GeO_2–doped vapor phase composition using a 60 cm long waveguide tube of dimension 20/17.5 mm where different parts of the soot deposit were soaked for different time span ranging from 15 to 60 minutes. The solution containing 0.3 M $AlCl_3$+0.01 M $ErCl_3$ made using ethanol was used for this experiment. The tube with the deposit was marked into different parts of equal length and during solution doping; the solution was partly drained out (at a fixed draining rate of 2.5 cm/min) after fixed time intervals from the deposited tube so that different portions of the deposit were soaked for different time periods. The input end from where the deposition took place was soaked for minimum time period while the other end of the tube was soaked for maximum time period. The experiments were performed using two different deposition temperature regimes namely at 1250±5°C and at 1300±5°C. Subsequent to solution soaking the soaked tube was processed further to obtain the final preform. Fibers were drawn from all the different parts and the incorporated Er-ion in different parts soaked for different time spans was evaluated to investigate the effect of dipping period on the final fiber composition.

4.2.4 Influence of Al/RE proportion

It has already been discussed under section 4.1 that codoping with Al_2O_3 helps to enhance the RE ion solubility in silica and restricts the evaporation of RE_2O_3 resulting in a uniform radial distribution of RE and Al in the preform core. Further Al doping improves the flat-gain characteristics of an Er doped fiber (EDF). However, Al-doping beyond a certain limit gives rise to phase-separation and generation of defect centres at the core-clad boundary

(star-like pattern) leading to enhancement of scattering loss. So it is essential to find out suitable Al/RE proportion to fabricate preform/fibers of improved performance. Accordingly a series of preform runs were carried out by maintaining optimized vapor phase composition (to deposit GeO_2-doped silica soot) and other processing parameters by changing the solution composition from run to run. The porous core layer deposition temperature was fixed at 1250±5°C and 1300±5°C in two different series. In these experiments, preform runs were carried out by changing the solution composition where for a fixed Er concentration of 0.01 M, the Al/Er proportion was varied from 0 to 100 with several intermediate values. Preform runs with the soaking solution comprising only 0.01 M $ErCl_3$ in ethanol corresponding to Al/Er ratio of 0 was carried out to investigate the incorporation of Er ion in absence of Al ion. Subsequent processing of the soaked porous deposit produced preforms/fibers with variation in Al/Er ratio.

4.2.5 Core-clad interface problem

Formation of defects ('star-like' pattern) along core-clad interface is a universal phenomenon that occurs in Al_2O_3 rich preform/fiber core. The effect becomes more adverse in presence of GeO_2 in the core region. The presence of such defects results in unwanted scattering loss in the ultimate fiber. Although many investigations have been carried out by different groups to explain the origin of this defect and possible route to overcome the problem [An et al. 2004], no one has been able to suggest a reliable method to eliminate it. It is believed that viscosity mismatch between core-clad material is important factor responsible for this phenomena.

A novel approach that has been adopted in the present investigation in getting rid of this problem is employing a soaking solution containing dispersed fumed silica instead of conventional soaking solution. The amount of dispersed fumed silica (Alfa Aesar, surface area 175-200 m^2/gm) was varied in different preform runs from 0.1 to 0.6 gm based on Al-ion content of 0.3 to 1.75 M in the soaking solution. Both aqueous and alcoholic solutions were used to verify the effectiveness of the proposed process.

4.3 Characterization procedure

The characterization process used here is alike that discussed under section 3.2. The RI profiles of the fabricated preforms and ultimate fibers were evaluated using preform analyzer (PK2600) and fiber analyzer (NR-20). The concentration of Er was determined from the absorption peak at 980 nm in the spectral attenuation curve. The distribution of different dopants inside the preform/fiber core was evaluated using Electron Microprobe analysis. In addition, the core-clad interface boundary was observed under high resolution optical microscope to examine the defects formed, if any, due to addition of Al.

4.4 Results & discussion

4.4.1 Viscosity of solution and its influence

The measured value of viscosity reveals that solution viscosity increases with enhancement of solution strength as presented in Fig. 6. About 10 fold increase in viscosity value (1.98 to 19.5 cP) was observed for a variation in the concentration of $AlCl_3$ from 0.15 to 1.0 M in an ethanolic solution. Since the final RE concentration is proportional to the amount of solution retained by the porous structure, solution viscosity influences RE incorporation level in the final fiber. The solution retention capacity of the porous medium is dependent on viscosity

of the soaking solution [Kim et al. 2003] and equation (1) predicts that highly viscous solution requires longer infiltration time through porous medium. The solution retention is higher for high viscous solution. Thus based on the deposited soot layer morphology and its adhesion strength with glass surface, solution viscosity needs to be adjusted. For GeO_2 doped ($GeCl_4/SiCl_4$=0.86) silica soot layer deposited at a temperature in the region of 1200-1230°C porous structure shows good uniformity but its adhesion to silica glass surface is weak showing tendency of disengagement or crack development during solution doping stage if a solution of viscosity greater than 3.0 cP is used. In comparison, a soot layer of above composition deposited at a temperature region of 1260-1280°C shows good adhesion with no sign of imperfection for solutions up to a viscosity value of 7.0 cP. For solutions of higher viscosity it is essential to deposit the soot at temperatures above 1290°C. But the porosity decreases appreciably leading to poor rare earth incorporation. This is also accompanied by formation of larger pores having enhanced probability of local composition variation. Considering the above factors, a temperature of 1260°C is found to be optimum for deposition of SiO_2-GeO_2 (10.5 mol% GeO_2) core layer. The deposit can be used for solution impregnation without problem up to a solution strength of 0.60 M $AlCl_3$ in ethanol and leads to a NA of 0.20 or greater.

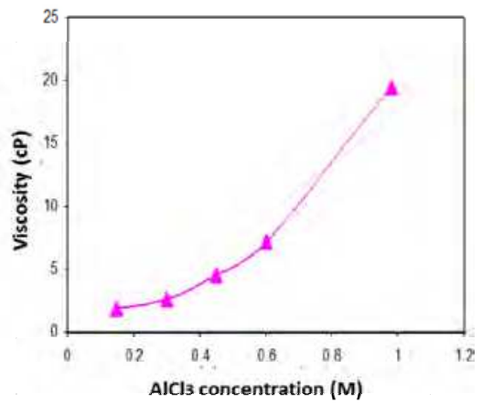

Fig. 6. Variation of Viscosity with changes in $AlCl_3$ concentration in ethanol.

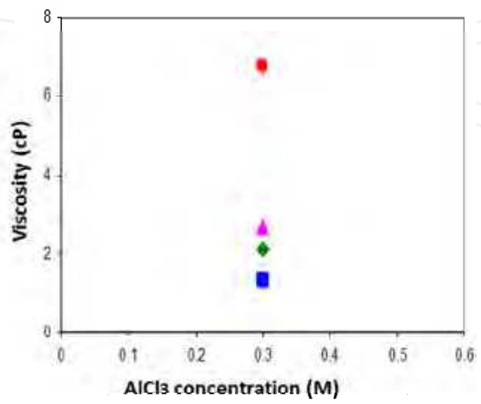

Fig. 7. Variation of Viscosity with change in solvent ● (propanol) ▲ (ethanol) ◆ (methanol) ■ (water).

4.4.2 Selected solvent vs. RE incorporation level

The nature of solvent is found to play a significant role on solution characteristics especially on viscosity as evident from Fig. 7 which shows the viscosity of a 0.3 M $AlCl_3$ solution increases from 1.3 cP to 6.7 cP by changing the solvent from water to propanol. It has been observed that for fibers obtained using a solution of 0.3 M $AlCl_3$+0.01 M $ErCl_3$ soaked for 60 minute, Er concentration difference equal to 120 ppm occurs between an ethanolic solution and an aqueous solution as evident from the spectral attenuation curve presented in Fig.8.

EPMA result [Fig.9] indicated that additional Al ion was adsorbed by alcohol soaked preform part compared to aqueous counterpart (preform part soaked with aqueous solution). This can be explained on the basis of surface tension differences of alcoholic and aqueous solution. The surface tension of fixed strength of aqueous solution selected for the study is found to be 2 to 3 times higher than that of the ethanolic solution. It has been reported [Khopin et al. 2005] that higher infiltration time is required for aqueous solution compared to alcoholic solution as a consequence of higher surface tension of aqueous solution.

Since Al and RE salts formed different complexes when added in solvents such as water or ethanol, size of the complex formed also governs the rate of dopant ion adsorption during solution impregnation. Due to the smaller size of the Al complex [Al $(OC_2H_5)x.Cl_{3-x}$] in alcohol compared to complex formed in aqueous solution $[Al(OH)(H_2O)_5]^{2+}$, porous deposit will soak more dopant ions during soaking in alcoholic solution compared to the aqueous solution.

Thus lower surface tension as well as smaller complex size of dopant ions are responsible for faster soaking in case of ethanolic solution compared to same strength of aqueous solution when soaked for fixed time span. The investigation reveals that solvent plays an important role in controlling incorporation of RE ion in fiber. Using water as solvent, longer soaking period is required to achieve saturation of pores and the pore size influence becomes greater compared to ethanolic solution of same concentration.

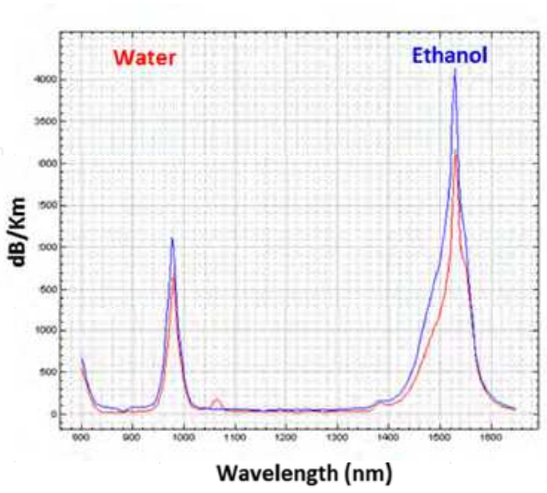

Fig. 8. Attenuation curve of fibers fabricated by using aqueous and ethanolic solutions of 0.3 M $AlCl_3$+0.01 M $ErCl_3$.

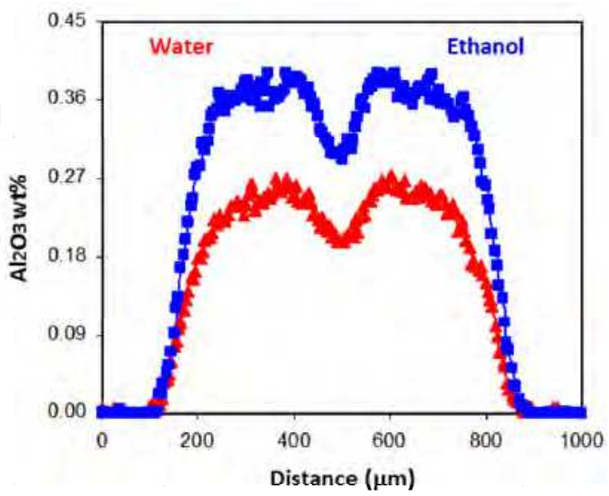

Fig. 9. EPMA result showing Al distribution across the preform core using aqueous and ethanolic solutions of 0.3 M $AlCl_3$+0.01 M $ErCl_3$.

4.4.3 RE incorporation level against dipping period

Conventionally dipping period of 1 hour is used in the solution doping process to achieve the saturation level during soaking stage but our investigation points out an interesting trend. From the above set of experiments, it is realized that the optimum dipping period is dependent on soot layer thickness, composition, porosity and also on solution characteristics like nature of solvent and Al/RE concentration. Accordingly, the dipping period can be suitably adjusted for getting a specific rare earth ion concentration in the sintered core layer. It is observed that during soaking, initially the rare earth incorporation rate is high, which decreases with time before getting saturated, depending upon soot morphology and solution nature. The variation in final rare earth ion concentration with dipping period when plotted produces Fig. 10 where effect of deposition temperature is clearly revealed. At 1250°C, the Er incorporation is nearly 300 ppm for a dipping period of 15 minutes which increases about 2 fold (~ 640 ppm) after a time period of 45 minutes. The maximum concentration after 60 minutes of dipping is about 690 ppm. The RE incorporation at various dipping periods is much lower at deposition temperature of 1300°C because of lower porosity of the porous deposit. Thus the investigation helps to obtain an optimized dipping period of 45 minute for a porous germanosilicate core layer having about 7.5 μm thickness, deposited at 1250-1260°C. This would correspond to an Er ion concentration of about 650 ppm when 0.3 M $AlCl_3$ + 0.01 M $ErCl_3$ solution in ethanol is used for soaking purpose. This observation essentially indicates presence of equilibrium between bulk solution and adsorbed dopant ion.

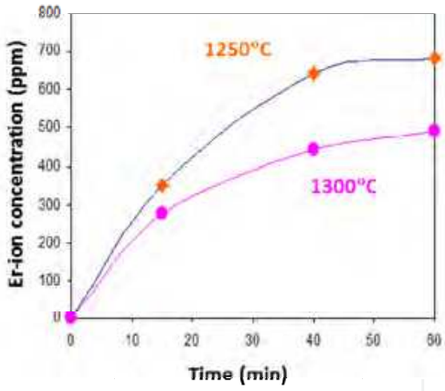

Fig. 10. Variation of Er ion concentration in the core with change in dipping period at deposition temperatures of 1250°C and 1300°C.

4.4.4 Influence of Al/RE proportion

Another important parameter under present investigation is the judicious selection of Al/RE proportion. It was observed that adjustment in Al proportion in the solution not only alters the Al incorporation but also RE^{3+} concentration in the fiber. Thus for deposited layers of fixed composition and porosity, it is possible to vary the final RE^{3+} concentration in the glass by maintaining the same RE ion concentration in the soaking solution with only adjustment in the Al ion proportion. This step is also responsible for controlling Al^{3+} concentration in the core. The observation is completely new and important. Usually, in order to change the RE concentration in the core, either the porosity is varied by changing soot composition or by altering the deposition temperature, otherwise the RE concentration in the soaking solution is adjusted proportionately. Fig. 11 represents the variation of Er concentration in final fiber using a fixed concentration of 0.01 M $ErCl_3$ but different $AlCl_3$ concentrations in the soaking solution for soot layer deposited at temperatures of 1250°C and 1300°C. The result indicates that the increase in $AlCl_3$ concentration in the solution from 0.1 M to 0.6 M leads to about 60% increase in Er ion incorporation. The RE incorporation for a fixed Al concentration can also be increased further by increasing the amount of RE salt in the soaking solution. The method provides much better control over RE incorporation and its uniformity along the preform/fiber length compared to the known techniques. As a result, the reproducibility is also improved compared to the conventional methods. The chemistry behind this can be explained as follows. During soaking, the RE absorption efficiency is increased with increase of Al concentration because of a 'cooperative phenomenon'. The increase in Al ion concentration along with the RE ions in the porous deposit facilitates formation of SiO_2-Al_2O_3-RE_2O_3 network during sintering. The RE ions thus become embedded in silica network, and their evaporation/ diffusion during sintering and collapsing at high temperature decreases. The overall effect is an effective increase in RE ion concentration. The effect is linear up to an Al ion concentration of 0.65 M in the soaking solution and then follows a decreasing trend.

The cooperative phenomenon described above has also been explained by a theoretical model [Dhar et al. 2008]. The model is based on the assumption that apart from direct adsorption from the solution phase, whose rate will be proportional to the concentration in the solution and also to the fraction of uncovered surface, there is also a parallel cooperative adsorption, in which an adsorbed Al particle helps additional adsorption of dopant ions. Rate of this cooperative adsorption will be proportional to the following factors, namely

concentration of Al ions in solution, fraction of uncovered surface and also to the fraction of surface covered with Al species. Desorption rate will be proportional to the fraction of surface covered by Al species. However, when Al concentration in soaking solution exceeds a certain limit, the number of vacant surface sites decreases significantly resulting in decrease of Er incorporation. This observation was also experimentally verified.

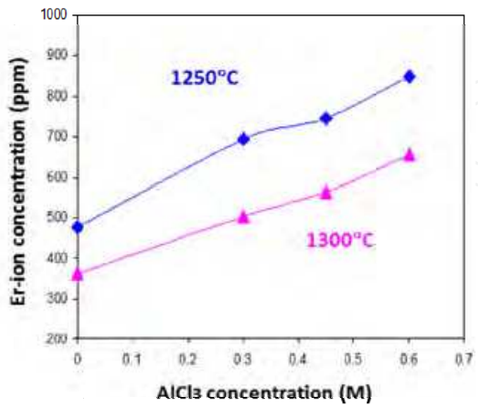

Fig. 11. Variation of Er ion concentration in the fiber with change in $AlCl_3$ concentration for a fixed $ErCl_3$ concentration in solution ▲ (1300°C) ◆ (1250°C).

4.4.5 Removal of core-clad interface defects

Use of dispersed fumed silica is found to be an excellent route to overcome the problem of defect generation (star-like pattern development) along the core-clad interface. The basis of the idea was to avoid segregation of Al-rich phase during sintering of soaked soot layer by providing free silica which helps to create alumino-silicate glass phase. Employing this technique about 4.6 wt% of Al_2O_3 containing preform in presence of GeO_2 (10.5 mol%) has been successfully fabricated without any core-clad interface disturbance. This preform was prepared using a solution containing about 1.75 M concentration of Al^{3+} ion where only 0.3 gm fumed silica was dispersed using ordinary ultra-sonication process [Dhar et al. 2010]. Figure 12 presents high resolution optical microscopic view of core-clad boundaries obtained employing (a) normal solution containing RE and Al salts without addition of fumed silica and (b) fumed silica dispersed soaking solution. It clearly shows how the addition of fumed silica has been effective in eliminating the defects formed due to the presence of high concentration of Al_2O_3 in the core.

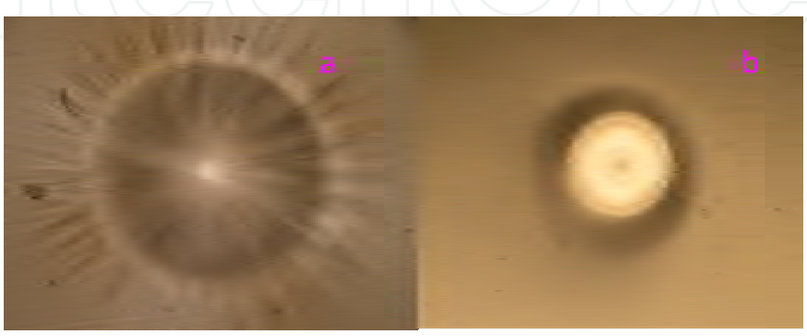

Fig. 12. Optical microscopic view of core-clad interface in preforms using (a) normal RE and Al containing solution and (b) fumed silica dispersed solution.

5. Correlation of different parameters

The overall investigation reveals the interdependence of soot layer characteristics with the solution properties and the dipping parameters. The soot composition and deposition temperature are found to significantly influence the porous layer microstructure which ultimately controls the amount of RE incorporation. Analysis of soot morphology and incorporated Er amount in final preform/fiber reveals existence of an empirical relation presented by a simple equation B=c.Q. Here "B" is Er ion absorption at 980 nm in dB/m, "c" a constant having value of 0.1 for the solution used in this experiment and "Q" pore area fraction (ratio of total pore area to the area of the deposit under SEM investigation). This analogy can be extended for other REs to predict the RE ion incorporation based on known soot parameters irrespective of soot composition. The viscosities of the solution are found to vary appreciably with change in solution strength and nature of solvent. About 10 fold increase in the viscosity is observed for a variation in the $AlCl_3$ concentration from 0.15 to 1.0 M in ethanolic solution. Thus the selection of solution of appropriate viscosity becomes an important criteria depending upon the porous soot layer morphology and its adhesion to the glass surface in order to avoid defects in the core. For GeO_2 doped ($GeCl_4/SiCl_4$=0.86) silica soot layer deposited at temperature in the region of 1260-1280°C, the porous structure shows good adhesion with little sign of imperfection for solution up to a viscosity of 7.0 cP. An important effect first time observed is the interdependence of Al ion concentration with the RE incorporation into the core because of a cooperative phenomenon. Thus for deposited layers of fixed composition and porosity, it is possible to vary the final RE^{3+} concentration in the glass by maintaining the same RE ion concentration in the soaking solution, with only adjustment in the Al ion proportion. It is also possible to adjust the average RE concentration to the desired levels by appropriate selection of dipping period. A soaking period of 45 minute is observed to be optimum for a porous core layer of 7.5 μm thickness, as the incorporation rate slows down appreciably after this period. Thus for fabricating a germanosilicate core fiber with numerical aperture of 0.20 or above, a process condition, where the porous core is deposited maintaining 1250-1260°C temperature, the soaking solution contains 0.3 M $AlCl_3$+ 0.01 M $ErCl_3$ made in ethanol and dipping time is selected as 45 minute, is observed to be optimum and the fiber core is found to contain around 650 ppm of Er^{3+} ion with appreciably good doping uniformity along the length. Several preforms and fibers with good reproducibility have been fabricated by the above process.

6. Conclusion

The influence of parameters associated with different phases of the solution doping process viz. soot deposition by MCVD technique and RE impregnation via solution doping method has been revealed through a systematic investigation. This has led to optimization of fabrication conditions to achieve better control over RE incorporation and enhanced repeatability. Experimental results indicate strong interdependence of soot morphology and solution doping parameters with ultimate preform/fiber properties. For the first time, the influence of the parameters has been exposed in a quantitative manner. The cooperative phenomenon not observed earlier between Al and RE offers a new approach of controlling RE concentration in the core. The method provides better control over RE incorporation and its uniformity along the preform/fiber length compared to the known technique. A process

reproducibility of about 80% has been achieved by maintaining the optimized fabrication conditions.

7. References

Ainslie, B. J., Armitage, R., Craig, S. P. & Wakefield, B. (1988), Fabrication and optimization of the erbium distribution in silica based doped fibres, *Proceedings of ECOC*, p. 62, Brighton, UK, September 1988

An, H., Tang, Y., McNamara, P. & Fleming, S. (2004), Viewing structural inhomogeneities at the core-cladding interface of re-heated MCVD optical fibre preforms with optical microscopy, *Optics Express,* Vol. 12, No. 25, (December 2004), pp. 6153-6158, ISSN 1094-4087

Arai, K., Namikawa, H., Kumata, K. & Honda, T. (1986), Aluminum or phosphorous co-doping effects on the fluorescence and structural properties of neodymium-doped silica glass, *Journal of Applied Physics*, Vol. 59, (January 1986), pp. 3430-3436, ISSN 0021-8979

Becker, P. C., Olsson, N. A., & Simpson, J. R. (1999), *Erbium doped fiber amplifiers-Fundamentals and technology* (1st Edition), Academic Press, ISBN 978-0-12-084590-3, San Diego, CA USA

Bandyopadhyay, T., Sen, R., Bhadra, S.K., Dasgupta, K. & Paul M. (2001), Process for making rare earth doped optical fibre, US Patent 6,751,990, 6.22.2004, Available from http://www.freepatentsonline.com/6751990.html

Chatterjee, M., Sen, R., Pal, M., Naskar, M., Paul, M., Bhadra, S., Dasgupta, K., Ganguli, D., Bandyopadhyay, T., Gedanken, A. & Reisfeld, R. (2003), Rare-earth doped optical fibre from oxide nano-particles, *Acta Optica Sinica*, Vol. 23, (October 2003), pp. 35-56, ISSN 0253-2239

Dhar, A., Paul, M. C., Pal, M., Mondal, A. Kr., Sen, S., Maiti, H. S. & Sen, R. (2006), Characterization of porous core layer for controlling rare earth incorporation in optical fiber, *Optics Express*, Vol. 14, No. 20, (October 2006), pp. 9006-9015, ISSN 1094-4087

Dhar, A., Paul, M. C., Pal, M., Bhadra, S. K., Maiti, H. S. & Sen, R. (2007), An improved method of controlling rare earth incorporation in optical fiber, *Optics Communication*, Vol. 277, (September 2007), pp. 329-334, ISSN 0030-4018

Dhar, A., Pal, A., Paul, M. Ch, Ray, P., Maiti, H. S. & Sen, R. (2008), The mechanism of rare earth incorporation in solution doping process, *Optics Express*, Vol. 16, No. 17, (August 2008), pp. 12835-12846, ISSN 1094-4087

Dhar, A., Das, S., Maiti, H.S. & Sen, R. (2010), Fabrication of high aluminium containing rare-earth doped fiber without core-clad interface defects, *Optics Communication*, Vol. 283. pp. 2344-2349, ISSN 0030-4018

Digonnet, M. J. F. (1993), *Rare Earth Doped Fiber Lasers and Amplifiers* (2nd Edition), Marcel Dekker Inc., ISBN 0824704584, New York, USA

Digiovanni, D. J., Macchesney, J. B. & Kometani, T. Y. (1989), Structure and properties of silica containing aluminum and phosphorus near the $AlPO_4$ join, *Journal of Non-Crystalline Solids*, Vol. 113, (November 1989), pp. 58-64, ISSN 0022-3093

Khopin, V. F., Umnikov, A. A., Gur'yanov, A. N., Bubnov, M. M., Senatorov, A. K. & Dianov, E. M. (2005), Doping of optical fiber preforms via porous silica layer

infiltration with salt solution, *Inorganic Materials,* (Engl. Transl), Vol. 41, No. 3, (March 2005), pp. 303-307, ISSN 1608-3172

Kim, Y. H., Paek, U. C. & Han, W. T. (2001), Effect of soaking temperature on concentrations of rare-earth ions in optical fibre core in solution doping process, *Proceedings of Rare-earth-doped materials and DevicesV, SPIE*, Vol. 4282, ISBN 9780819439604, San Jose, CA, USA, January 2001

Laoulacine, R., Morse, T. F., Charilaou, P. & Cipolla, J. W. (1988), Aerosol delivery of non-volatile dopants in the MCVD System, Extended Abstracts of the AIChE Annual Meeting, Washington, DC, USA, December, 1988

MacChesney, J. B. & Simpson, J. R. (1985), Optical waveguides with novel compositions, *Proceedings of Optical Fibre Communication Conference*, Paper WH5, p. 100, Technical Digest, San Diego, CA, USA, February, 1985

MacChesney, J. B. (2000), MCVD: Its origin and subsequent developments, *IEEE Journal of Quantum Electronics*, Vol. 6, (December 2000), pp. 1305-1306, ISSN 0018-9197

Matejec, V., Hayer, M., Pospisilova, M. & Kasik, I. (1997), Preparation of optical cores of silica optical fiber by the sol-gel method, *Journal of Sol-Gel Science Technology*, *V*ol.8, (February 1997), pp. 889-893, ISSN 1573-4846

Mears R. J., Reekie, L., Jauncey, I. M., & Payne, D. N. (1987), Low-noise Erbium-doped fiber amplifier at 1.54μm, *Electronics Letter*, Vol. 23, pp. 1026-1028, ISSN 0013-5194

Morse, T. F., Reinhart, L., Kilian, A., Risen, W. & Cipolla, J. W (1989), Aerosol doping technique for MCVD and OVD, *Proceedings of Fibre Laser Sources and Amplifiers, SPIE*, Vol. 1171, pp. 72-79, ISBN 9780819402073

Mukhopadhyay, S. S. & Kundu, D. (2006), Chemical composition analysis of germinate glass by alkalimetric titration of Germinate Mannitol complex, *Journal of Indian Chemical Society*, Vol. 83, No. 3, (March 2006), pp. 255-258. ISSN 0019-4522

Nagel, S. R., MacChesney, J. B. & Walker, K. L. (1982), Overview of the Modified Chemical vapour Deposition (MCVD) process and performance, *IEEE Journal of Quantum Electronics*, Vol. QE-18, No. 4, (April 1982), pp. 459-476, ISSN 0018-9197

Pal, M., Sen, R., Paul, M. C., Bhadra, S. K., Chatterjee, S., Ghosal, D. & Dasgupta, K. (2005), Investigation of the deposition of porous layers by the MCVD method for the preparation of rare-earth doped cores of optical fibers, *Optics Communications*, Vol. 254, (October 2005), pp. 88-95, ISSN 0030-4018

Poole, S. B., Payne, D. N. & Fermann, M. E. (1985), Fabrication of low-loss optical fibres containing rare earth ions, *Electronics Letter*, Vol. 21, No. 17, (August 1985), pp. 737-738, ISSN 0013-5194

Poole, S. B., Payne, D. N., Mears, R. J., Fermann, M. E. & Laming, R. I. (1986), Fabrication and characterization of low-loss optical fibres containing rare-earth ions, *Journal of Lightwave Technology,* Vol. LT-4, No. 7, (July 1986), pp. 870-876, ISSN 0733-8724

Stone, J. & Burrus, C. A. (1973), Nd^{3+} doped SiO_2 lasers in end pumped fiber geometry, *Applied Physics Letters*, Vol. 23, (October 1973), pp. 388-389, ISSN 1077-3118

Tammela, S., Kiiveri, P., Sarkilahti, S., Hotoleanu, M., Vaikonen, H., Rajala, M., Kurki, J. & Janka, K. (2002), Direct Nanoparticle Deposition process for manufacturing very short high gain Er-doped silica glass fibers, *Proceedings of ECOC 2002*, ISBN 8790974638, Copenhagen, September, 2002

Thompson, D. A., Bocko, P. L. & Gannon, J. R. (1984), New source compounds for fabrication of doped optical waveguide fibres, *Proceedings of Fibre Optics adverse Environment II*, SPIE, Vol. 506, ISBN 9780892525416

Tingye, L. (1985), *Optical Fiber Communications Volume 1 Fiber Fabrication,* Academic Press, Inc., ISBN 0124473016, Orlando, Florida.

Townsend, J. E., Poole, S. B. & Payne, D. N. (1987), Solution-doping technique for fabrication of rare-earth-doped optical fibers, *Electronics Letters*, Vol. 23, No. 7, (March 1987), pp. 329-331, ISSN 0013-5194

Tumminelli, R. P., McCollum, B. C. & Snitzer, E. (1990), Fabrication of high-concentration rare-earth doped optical fibres using chelates, *Journal of Lightwave Technology*, Vol. LT-8, No. 11, (November 1990), pp. 1680-1683, ISSN 0733-8724

IntechOpen

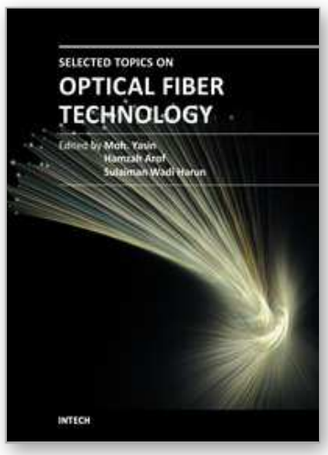

Selected Topics on Optical Fiber Technology

Edited by Dr Moh. Yasin

ISBN 978-953-51-0091-1

Hard cover, 668 pages

Publisher InTech

Published online 22, February, 2012

Published in print edition February, 2012

This book presents a comprehensive account of the recent advances and research in optical fiber technology. It covers a broad spectrum of topics in special areas of optical fiber technology. The book highlights the development of fiber lasers, optical fiber applications in medical, imaging, spectroscopy and measurement, new optical fibers and sensors. This is an essential reference for researchers working in optical fiber researches and for industrial users who need to be aware of current developments in fiber lasers, sensors and other optical fiber applications.

How to reference

In order to correctly reference this scholarly work, feel free to copy and paste the following:

Ranjan Sen and Anirban Dhar (2012). An Improved Method of Fabricating Rare Earth Doped Optical Fiber, Selected Topics on Optical Fiber Technology, Dr Moh. Yasin (Ed.), ISBN: 978-953-51-0091-1, InTech, Available from: http://www.intechopen.com/books/selected-topics-on-optical-fiber-technology/an-improved-method-of-fabricating-rare-earth-doped-optical-fiber

INTECH
open science | open minds

InTech Europe
University Campus STeP Ri
Slavka Krautzeka 83/A
51000 Rijeka, Croatia
Phone: +385 (51) 770 447
Fax: +385 (51) 686 166
www.intechopen.com

InTech China
Unit 405, Office Block, Hotel Equatorial Shanghai
No.65, Yan An Road (West), Shanghai, 200040, China
中国上海市延安西路65号上海国际贵都大饭店办公楼405单元
Phone: +86-21-62489820
Fax: +86-21-62489821

© 2012 The Author(s). Licensee IntechOpen. This is an open access article distributed under the terms of the Creative Commons Attribution 3.0 License, which permits unrestricted use, distribution, and reproduction in any medium, provided the original work is properly cited.

IntechOpen

IntechOpen